FEBS Open Bio 3 (2013) 89–100

journal homepage: www.elsevier.com/locate/febsopenbio

The sea urchin metallothionein system: Comparative evaluation of the SpMTA and SpMTB metal-binding preferences☆

Mireia Tomas[a,b], Jordi Domènech[b], Mercè Capdevila[a], Roger Bofill[a,*], Sílvia Atrian[b]

[a] Departament de Química, Facultat de Ciències, Universitat Autònoma de Barcelona, Cerdanyola del Vallès, 08193 Barcelona, Spain
[b] Departament de Genètica, Facultat de Biologia, Universitat de Barcelona, Av. Diagonal 645, 08028 Barcelona, Spain

ARTICLE INFO

Article history:
Received 10 December 2012
Received in revised form 9 January 2013
Accepted 9 January 2013

Keywords:
Metallohionein
Echinodermata
Cadmium
Copper
Zinc

ABSTRACT

Metallothioneins (MTs) constitute a superfamily of ubiquitous metal-binding proteins of low molecular weight and high Cys content. They are involved in metal homeostasis and detoxification, amongst other proposed biological functions. Two MT isoforms (SpMTA and SpMTB) have been reported in the echinoderm *Strongylocentrotus purpuratus* (sea urchin), both containing 20 Cys residues and presenting extremely similar sequences, although showing distinct tissular and ontogenic expression patterns. Although exhaustive information is available for the Cd(II)-SpMTA complex, this including the full resolution of its 3D structure, no data has been reported concerning either SpMTA Zn(II) and Cu(I) binding properties, or the characterization of SpMTB at protein level. In this work, both the SpMTA and SpMTB isoforms, as well as their separate α and β domains, have been recombinantly synthesized in the presence of Zn(II), Cd(II) or Cu(II), and the corresponding metal complexes have been analyzed using electrospray mass spectrometry, and CD, ICP-AES and UV–vis spectroscopies. The results clearly show a better performance of isoform A when binding Zn(II) and Cd(II), and of isoform B when coordinating Cu(I). Thus, our results confirm the differential metal binding preference of SpMTA and SpMTB, which, together with the reported induction pattern of the respective genes, highlights how also in Echinodermata the MT polymorphism may be linked to the evolution of different physiological roles.

1. Introduction

Metallothioneins (MTs) are a superfamily of universal and ubiquitous low molecular weight proteins that bind essential and toxic metal ions through their abundant Cys residues, forming multinuclear metal–thiolate clusters. They are involved in many crucial biological processes, such as metal homeostasis and detoxification, or oxidative stress protection, among others [1]. Although their protein sequences are dramatically heterogeneous and consequently their classification is not a trivial affair, their metal-binding behavior converges to either Zn-thioneins, which show a binding preference for divalent metal ions, or Cu-thioneins, with an optimized coordination of monovalent metal ions [2]. Beyond this simplistic dual model, the comprehensive consideration of the metal-binding features of a huge number of MT peptides later led to the proposal of a continuous gradation between both extreme behaviors [3]. Unfortunately, the sequence determinants of the metal specificity of MTs are still unknown [4], although it should be considered a key element for a better understanding of the evolutive differentiation [5] and physiological function of these peculiar metalloproteins [6]. Polymorphism is one of the most significant features of MTs, since at least all the eukaryote organisms studied until now exhibit MT systems composed of almost similar paralog forms [5]. Ideally, each isoform would correspond to a definite physiological function, but it is plainly evident that in most cases ontogenic, tissular and/or functional differentiation has not been achieved, so that no clear correlation exists between multiple MT isoforms and their *in vivo* performance.

In this scenario, and with the aim of gathering data on the most prominent model organisms, we undertook the characterization of the metal-binding preferences of the purple sea urchin (*Strongylocentrotus purpuratus*, echinoderm) MT isoforms. Echinodermata constitute a very interesting phylum since, as the unique invertebrate deuterostomes, they are evolutively close to the Chordates, which are also deuterostomes (for a recent review on Echinodermata MTs, see [7]). At genomic level, seven different homologous MT genes have been reported in *S. purpuratus*, of which only three produce biologically relevant isoforms: *SpMTA* and the pair $SpMTB_1$–$SpMTB_2$, the latter encoding proteins with identical sequence [8–10]. Significantly,

* Corresponding author. Address: Unitat Química Inorgànica, Departament de Química, Facultat de Ciències, Universitat Autònoma de Barcelona, Bellaterra 08193, Catalonia, Spain. Tel.: +34 935812886; fax: +34 935812477.
E-mail address: Roger.Bofill@uab.cat (R. Bofill).

2211-5463/$36.00
http://dx.doi.org/10.1016/j.fob.2013.01.005

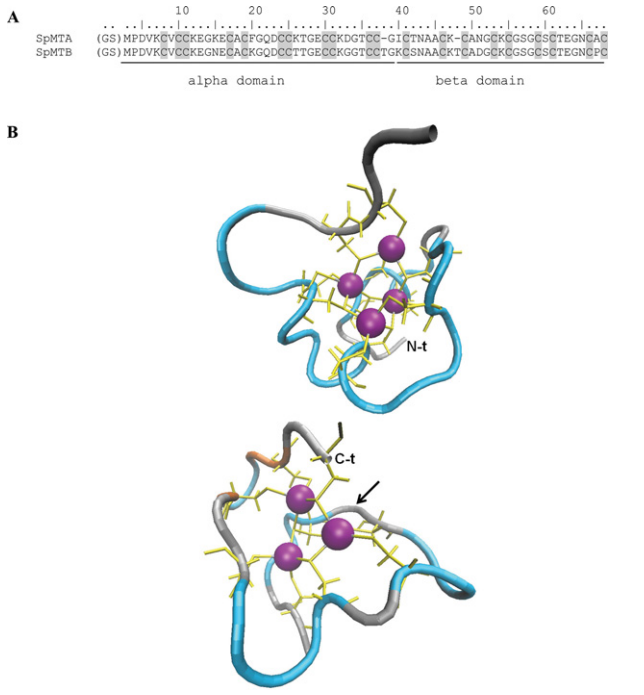

Fig. 1. (A) Amino acid sequence alignment of recombinant SpMTA and SpMTB. Note that the N-term Gly–Ser residues derive from the GST-fusion system used for recombinant synthesis and purification. (B) 3D structures of Cd_4-αSpMTA (top) and Cd_3-βSpMTA (bottom) generated from PDB files 1QJK and 1QJL, respectively, with VMD software (http://www.ks.uiuc.edu/Research/vmd/) [Humphrey W, Dalke A, Schulten K. VMD – visual molecular dynamics. J. Molec. Graphics 1996;14:33–38]. Color code: random coil, silver; turn, cyan; extended beta, orange; Cd(II) ions, purple; Cys residue backbone and Cys-Cd connectivities, yellow. N-term and C-term ends of SpMTA sequence are indicated, and an arrow marks the position of the insertion of a Thr residue in SpMTB. (For interpretation of the references to color in this figure legend, the reader is referred to the web version of this article.)

SpMTA and *SpMTB* exhibit different quantitative tissular and temporal expression patterns. Hence, *SpMTA* is transcribed in ectodermal tissues, while *SpMTB* is expressed in both the ectodermal and endodermal structures. Both genes are constitutively expressed, and under physiological conditions *SpMTA* mRNA levels reach up to 10 times those of *SpMTB*. However, under metal (zinc or cadmium) overload, *SpMTB* expression is further induced, so that SpMTB achieves protein levels similar to those of SpMTA [8,10].

SpMTA is a 64-amino acid peptide including 20 Cys, while the SpMTB sequence is two amino acids longer, with fully conserved Cys and only 10 residue substitutions (Fig. 1(A)), although some other changes have been detected in minor EST clones, attributable to natural polymorphism. Of both isoforms, only the study of SpMTA has attracted great interest, since the Cys–Cys motifs typical of the C-terminal moiety (or α domain) of the mammalian MTs are located here in the N-terminal moiety, and *vice versa* for the Cys–X–Cys motifs typical of the N-terminal half (or β domain) of the mammalian MTs (Fig. 1(A)). This inverted arrangement led to propose a specific evolutionary theory for the origin of different MT proteins, based on considering the number and position of the binding domains in different MTs [11]. Thereafter, several structural features of the Cd-SpMTA complexes were revealed by the work in the laboratory of Prof. Kägi on recombinant SpMTA [12–14], which culminated with the determination of the three-dimensional structure of reconstituted-$^{113}Cd_7$-SpMTA, solved by NMR in 1999 (Fig. 1(B)) [15]. These results confirmed that the global structure of each Cd_7-SpMTA domain resembled that of the mammalian MTs, although a significantly different connectivity pattern of the Cd–S bonds and novel local polypeptide folds arose in SpMTA. Precisely, two globular domains separated by a flexible hinge and encompassing a $Cd_4(SCys)_{11}$ and a $Cd_3(SCys)_9$ cluster in an inverted order with respect to mammalian MTs were encountered. The $Cd_4(SCys)_{11}$ cluster (in the N-term protein α domain) consisted of the union of 2 six-membered rings sharing 2 Cd–S bonds, thus including 5 bridging and 6 terminal S atoms, whereas the $Cd_3(SCys)_9$ cluster (in the C-term protein β domain) consisted of 3 cadmium ions and 3 bridging Cys thiolates forming a six-membered ring, while the other six Cys acted as terminal ligands. Although it was not possible to determine the mutual orientation of the two domains, it was evident that both were twisted to the left around the metal–thiolate cluster. This constrasts with the mammalian MT complexes, where the β domain is wrapped with right-handed chirality, thus representing the only known example of left-handed β domain.

This exhaustive information on the complexes yielded by SpMTA upon divalent metal ion coordination contrasts with the null information about its copper binding abilities nor about metal ion handling by SpMTB. Therefore, in order to gain an insight into the evolutive significance of the two different MT isoforms in sea urchin, we aimed at performing a comparative study of their metal ion coordination features. To this end, this work describes the Zn(II), Cd(II) and Cu(I)-binding abilities of recombinant SpMTA and SpMTB, as well as of their separate domains, in order to determine their metal binding behavior and preferences. The consideration of all the obtained results is consistent with a higher Zn/Cd-thionein character for SpMTA, and a better performance of SpMTB when binding copper, and they confirm that a slight but consistent difference between the physiological functions of both isoforms may be envisaged.

2. Materials and methods

2.1. Cloning of MT cDNA constructs

All the metal-MT complexes investigated in the present study were recombinantly synthesized in *Escherichia coli* through cloning of their coding sequences into the pGEX-4T1 plasmid (GE Healthcare, Little Chalfont, UK) to yield primary glutathione S-transferase (GST)-MT fusions from which the corresponding metal-MT complexes were subsequently purified [16,17]. The SpMTA cDNA was kindly provided by Prof. Kägi and subsequently cloned into the pGEX-4T1 *Bam*HI/*Sal*I restriction sites added by PCR amplification, using 5′-CCCGGATCCATGCCTGATGTCAAG-3′ as upstream primer and 5′-GCGCCCGTCGACCTAGCATGCACA-3′ as downstream primer. According to the reported SpMTA domain boundaries [15], cDNAs encoding for its separate moieties were obtained by PCR reactions that added *Bam*HI/*Xho*I restriction sites with the following oligonucleotides: for the N-terminal fragment or α domain (encompassing residues 1–36 of the full polypeptide), 5′-CCCGGATCCATGCCTGATGTCAAG-3′ (upstream) and 5′-AAACTCGAGTCATCCACAGCAGGTTCCATCCTTG-3′ (downstream); and for the C-terminal fragment or β domain (residues 37–64 of the full polypeptide), 5′-ACACACGGATCCATATGCACAAACGCTGCATGC-3′ (upstream) and 5′-AAACCCCTCGAGCTAGCATGCACAGTTCCCCTC-3′ (downstream). The cDNA of the SpMTB isoform was obtained from the Sea Urchin Genome Project Library Collection, in the California Institute of Technology (Caltech), and corresponded to the EST clone PMC_62379562 (seq ID NCBI 214576). The corresponding ORF was amplified by a PCR reaction that added *Bam*HI/*Xho*I restriction sites to the respective 5′ and 3′ ends of the coding sequence, using the purified cDNA of the EST clone as template and the following primers: 5′-CCCGGATCCATGCCTGATGTCAAGTGTGTCTGC-3′ (upstream) and 5′-AAACCCCTCGAGCTAGCATGGACAGTTCCCCTC-3′ (downstream). Based on the reported domain boundaries of SpMTA [15], cDNAs encoding for the separate SpMTB

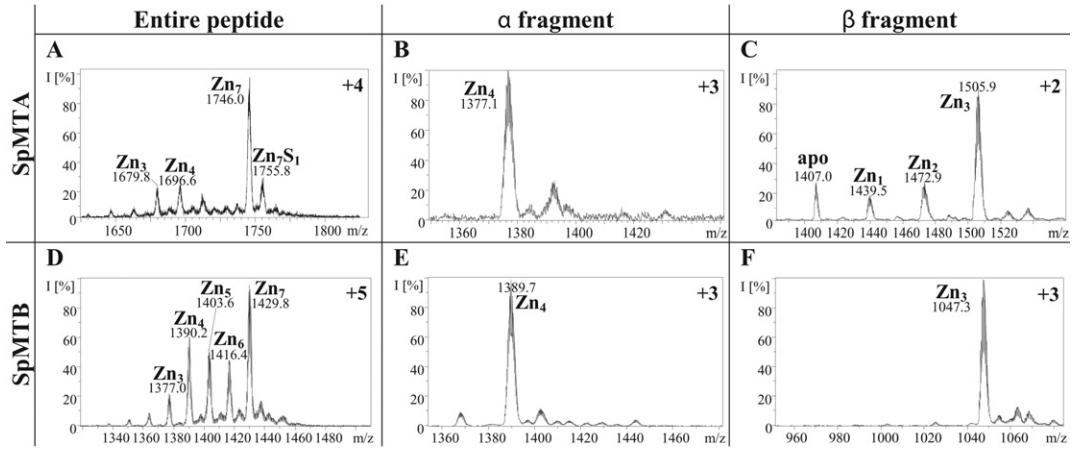

Fig. 2. Representative charge states for the ESI-MS spectra recorded at pH 7.0 of recombinant Zn-SpMTA (A), Zn-αSpMTA (B), Zn-βSpMTA (C), Zn-SpMTB (D), Zn-αSpMTB (E) and Zn-βSpMTB (F). The observed species are collected in Table 2.

moieties were obtained by PCR reactions with the following oligonucleotides: for the N-terminal fragment or α domain (encompassing residues 1–37 of the full polypeptide), 5′-CCCGGATCCATGCCTGATGTCAAGTGTGTCTGC-3′ (upstream) and 5′-AAACTCGAGTCATCCAGTGCAGCAGGTTCCACC-3′ (downstream); and for the C-terminal fragment or β domain (residues 38–66 of the full polypeptide), 5′-ACACACGGATCCAAATGCTCAAATGCGGCATGC-3′ (upstream) and 5′-AAACCCCTCGAGCTAGCATGGACAGTTCCCCTC-3′ (downstream). All the PCR reactions consisted of 35-cycle amplifications, performed with 1.25 U of GoTaq DNA polymerase (Promega, Madison, USA), 0.25 mM dNTPs and 0.24 μM of the required primers at 2 mM $MgCl_2$ (final concentration), in a final volume of 100 μL, under the following cycle conditions: 30 s at 94 °C (denaturation), 30 s at 58 °C (hybridization) and 30 s at 72 °C (elongation). An initial denaturation step where samples were heated at 94 °C for 2 min ensured that the target DNA was completely denatured, and elongation conditions were maintained for 7 min after the 35 cycles. The final products were analyzed by agarose gel electrophoresis/GelRed Nucleic Acid Gel Stain (Biotium, Hayward, CA, USA) staining; the band with the expected size was excised and subcloned into the pGEX-4T1 vector. Before recombinant protein synthesis, all coding sequences were confirmed by automated DNA sequencing. To this end, the pGEX-derived constructs were transformed into *E. coli* MATCH I cells, and sequenced using the ABI PRISM BigDye Terminator v3.1 Cycle Sequencing Kit (Applied Biosystems, Foster City, CA, USA) in an ABI PRISM 310 Automatic Sequencer (Applied Biosystems, Foster City, CA, USA). In all cases, the expected sequence was corroborated.

2.2. Recombinant synthesis and purification of metal-MT complexes

The SpMTA-GST and SpMTB-GST fusion polypeptides and their respective separate α and β domains were biosynthesized in 5 L cultures of transformed protease-deficient *E. coli* BL21 cells. Expression was induced with isopropyl β-D-thiogalactopyranoside (IPTG) and cultures were supplemented with 500 μM $CuSO_4$, 300 μM $ZnCl_2$ or 300 μM $CdCl_2$ (final concentrations) and were allowed to grow for a further 3 h. In the case of Cu(II)-enriched cultures, both normal and low aeration conditions (N.A. and L.A., respectively) were assayed according to the procedure described elsewhere [18]. A total protein extract was prepared from these cells as previously described [16]. Metal complexes were recovered from the MT-GST fusion constructs by thrombin cleavage and batch-affinity chromatography using Glutathione-Sepharose 4B (General Electric HC). The metal complexes were finally purified through FPLC in a Superdex75 column (General Electric HC) equilibrated with 50 mM Tris–HCl, pH 7.0. Selected fractions were confirmed by 15% SDS–PAGE and kept at −80 °C until further use. All procedures were performed using Ar (pure grade 5.6) saturated buffers, and all syntheses were performed at least twice to ensure reproducibility. Further details on the purification procedure can be found in [16]. As a consequence of the cloning requirements, the dipeptide Gly–Ser was present at the N-terminus of all polypeptides; however, this had previously been shown not to alter the MT metal-binding capacities [17].

2.3. In vitro Cd- and Cu-binding studies

The titration of all Zn-MT complexes with Cd(II) or Cu(I) at pH 7 were carried out following the methodology previously described [19,20], using $CdCl_2$ or $[Cu(CH_3CN)_4]ClO_4$ solutions, respectively. The acidification/reneutralization experiments were also performed by adapting the procedure reported in [21]. Essentially, 10–20 μM preparations of the Cd-peptides were acidified from pH 7.0 to pH 1.0–2.0 with 1×10^{-3} M HCl. CD and UV–vis spectra were recorded at several pH values both immediately after acid addition and 10 min later, always with identical results. Finally, the samples were kept at pH 1.0–2.0 for 20 min and were then reneutralized with 1×10^{-3} M NaOH, and CD and UV–vis spectra were recorded at several pH values. In some cases, several molar equivalents of an aqueous solution of Na_2S were added to the reneutralized MT forms, with the aim of reproducing the original Cd-MT CD fingerprints. All results were corrected for dilution effects, and during all experiments strict oxygen-free conditions were kept by saturating all solutions with Ar.

2.4. Protein quantification and spectroscopic analyses

The S, Zn, Cd and Cu content of the Zn-, Cd- and Cu-MT preparations was analyzed by means of Inductively Coupled Plasma Atomic Emission Spectroscopy (ICP-AES) in a Polyscan 61E (Thermo Jarrell Ash) spectrometer, measuring S at 182.040 nm, Zn at 213.856 nm, Cd at 228.802 and Cu at 324.803 nm. Samples were treated as in [22], but were alternatively incubated in 1 M HCl at 65 °C for 5 min prior to measurements, in order to eliminate possible traces of labile sulfide ions, as otherwise described [23]. Protein concentrations were calculated from the acid ICP-AES sulfur measurement, assuming that all S atoms were contributed by the MT peptide. A Jasco spectropolarimeter (Model J-715) interfaced to a computer (J700 software) was used

Table 1
List of theoretical and experimental molecular weights (MW) corresponding to the apoforms of the six recombinantly synthesized polypeptides.

MT	Theoretical MW	Experimental MW
SpMTA	6532.0	6534.9 ± 0.8
αSpMTA	3874.0	3873.9 ± 0.4
βSpMTA	2820.2	2819.6 ± 0.5
SpMTB	6700.7	6698.6 ± 0.4
αSpMTB	3913.5	3912.4 ± 0.1
βSpMTB	2949.3	2948.6 ± 0.4

for CD measurements at a constant temperature of 25 °C maintained by a Peltier PTC-351S apparatus. Electronic absorption measurements were performed on an HP-8453 Diode array UV–vis spectrophotometer. All spectra were recorded with 1 cm capped quartz cuvettes, corrected for the dilution effects and processed using the GRAMS 32 Software.

2.5. Mass spectrometry

MW determinations were performed by electrospray ionization time-of-flight mass spectrometry (ESI-TOF MS) on a Micro Tof-Q instrument (Bruker) interfaced with a Series 1100 HPLC Agilent pump, equipped with an autosampler, all of which were controlled by the Compass Software. Calibration was attained with 0.2 g NaI dissolved in 100 mL of a 1:1 H_2O:isopropanol mixture. Samples containing MT complexes with divalent metal ions were analyzed under the following conditions: 20 μL of protein solution injected through a PEEK (polyether heteroketone) column (1.5 m × 0.18 mm i.d.), at 40 μL min^{-1}; capillary counter-electrode voltage 5 kV; desolvation temperature 90–110 °C; dry gas 6 L min^{-1}; spectra collection range 800–2000 m/z. The carrier buffer was a 5:95 mixture of acetonitrile:ammonium acetate/ammonia (15 mM, pH 7.0). Alternatively, the Cu-MT samples were analyzed as follows: 20 μL of protein solution injected at 30 μL min^{-1}; capillary counter-electrode voltage 3.5 kV; lens counter-electrode voltage 4 kV; dry temperature 80 °C; dry gas 6 L min^{-1}. Here, the carrier was a 10:90 mixture of acetonitrile:ammonium acetate/ammonia (15 mM, pH 7.0). For analysis of all recombinant MT molecular masses, 20 μL of the corresponding Zn-MT samples were injected under the same conditions described before, but using a 5:95 mixture of acetonitrile:formic acid pH 2.5 as liquid carrier, which caused the complete demetalation of the peptides. The same conditions were then used to remove Zn(II) ions from mixed-metal Zn, Cu-MT species in order to quantify their total Cu content.

3. Results and discussion

3.1. Integrity and identity of the recombinant polypeptides

The cDNAs coding for the SpMTA and SpMTB isoforms as well as for their separate domains were cloned into the pGEX-4T1 plasmid for peptide synthesis. DNA sequencing confirmed that all these constructs included no artifactual nucleotide substitutions, and that the respective coding sequences were cloned in the correct frame after the GST encoding fragment. Recombinant syntheses yielded MT peptides of which the identity, purity and integrity was confirmed by ESI-MS of the respective apoforms, obtained by acidification at pH 2.5 of the corresponding Zn-MT complexes. Hence, in each synthesis a unique peak was detected, in which the MW was consistent with the calculated MW of the respective recombinant MT peptide, including N-terminal Gly–Ser residues derived from the GST-fusion construct (Table 1).

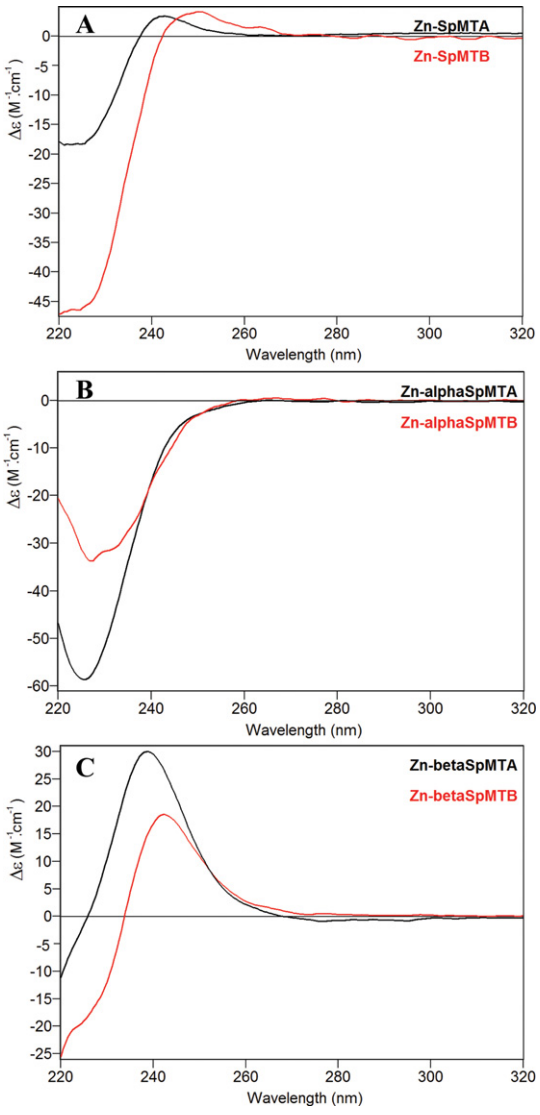

Fig. 3. CD spectra corresponding to the entire MT (A) and the separate constitutive α (B) and β (C) domains of SpMTA (black) and SpMTB (red) recombinantly synthesized in Zn-supplemented media. (For interpretation of the references to color in this figure legend, the reader is referred to the web version of this article.)

3.2. SpMTA exhibits better Zn(II) and Cd(II) binding abilities than SpMTB

Both SpMTA and SpMTB yield a major Zn_7-MT species when recombinantly synthesized as Zn(II)-complexes (Table 2, Fig. 2(A) and (D)), although the occurrence of several minor undermetalated, partially oxidized species is markedly significant for SpMTB, where all the species ranging from Zn_6 to Zn_3 are produced (Fig. 2(D)). This result already suggests a lower Zn^{II}-binding ability for SpMTB compared to SpMTA. The CD fingerprints of both Zn-preparations are similar and characteristic of Zn-MT complexes (Fig. 3(A)), and the *ca.* 10 nm red-shift of Zn-SpMTB is attributable to the differences between the respective β domains, as analyzed below.

When synthesized in the presence of Cd(II), SpMTA yields a major Cd_7 species (Fig. 4(A)), whose CD fingerprint shows an intense exciton coupling centered at 250 nm (Fig. 5(A)) typical of type A Cd-MT complexes [23], and which is also very similar to the CD spectrum previously reported for recombinant Cd_7-SpMTA [12,13]. Even though a

Table 2
Analytical characterization of recombinant SpMTA and SpMTB and their independent constitutive fragments synthesized in (A) Zn- and (B) Cd-enriched media.

MT	Concentration and metal/MT ratio[a]	ESI-MS[b]		
		Species (% abundance)	Theoretical MW	Experimental MW
A				
SpMTA	3.2×10^{-4} M 6.1 Zn	**Zn_7-SpMTA (100)**	6976.1	6978.8 ± 0.9
		Zn_7S_1-SpMTA (30)	7010.2	7016.5 ± 2.5
		Zn_4-SpMTA (20)	6786.0	6780.9 ± 0.2
		Zn_3-SpMTA (20)	6722.6	6715.9 ± 0.6
αSpMTA	0.9×10^{-4} M 3.8 Zn	**Zn_4-αSpMTA**	4127.5	4127.2 ± 0.1
βSpMTA	0.7×10^{-4} M 2.3 Zn	**Zn_3-βSpMTA (100)**	3010.3	3009.9 ± 0.1
		Zn_2-βSpMTA (30)	2947.0	2943.8 ± 1.5
		apo-βSpMTA (30)	2820.2	2811.0 ± 1.3
		Zn_1-βSpMTA (20)	2883.6	2877.0 ± 1.2
SpMTB	2.3×10^{-4} M 5.2 Zn	**Zn_7-SpMTB (100)**	7144.4	7143.5 ± 0.5
		Zn_6-SpMTB (50)	7081.0	7076.9 ± 1.3
		Zn_5-SpMTB (50)	7017.6	7012.9 ± 1.1
		Zn_4-SpMTB (60)	6954.3	6944.0 ± 0.9
		Zn_3-SpMTB (20)	6890.9	6880.0 ± 1.4
αSpMTB	2.2×10^{-4} M 3.8 Zn	**Zn_4-αSpMTB**	4167.0	4166.1 ± 0.1
βSpMTB	0.8×10^{-4} M 3.1 Zn	**Zn_3-βSpMTB**	3139.5	3138.9 ± 0.1
B				
SpMTA	0.7×10^{-4} M 7.7 Cd 0.0 Zn	**Cd_7-SpMTA (100)**	7305.3	7304.5 ± 0.5
		Cd_7S_1-SpMTA (20)	7339.4	7341.6 ± 1.8
αSpMTA	0.7×10^{-4} M 3.9 Cd 0.0 Zn	**Cd_4-αSpMTA**	4315.6	4316.1 ± 0.1
βSpMTA	0.2×10^{-4} M 2.8 Cd 0.4 Zn	**Cd_3-βSpMTA (100)**	3151.4	3151.8 ± 0.4
		Cd_3Zn_1-βSpMTA (30)	3214.8	3215.6 ± 0.6
SpMTB	0.8×10^{-4} M 6.7 Cd 0.0 Zn	**Cd_8-SpMTB (100)**	7583.9	7584.1 ± 0.5
		Cd_7S_2-SpMTB (50)	7541.6	7534.4 ± 0.9
		Cd_7-SpMTB (40)	7473.5	7474.8 ± 0.4
αSpMTB	1.3×10^{-4} M 4.0 Cd 0.0 Zn	**Cd_4-αSpMTB**	4355.1	4355.5 ± 0.4
βSpMTB	0.8×10^{-4} M 2.9 Cd 0.0 Zn	**Cd_3S_2-βSpMTB (100)**	3348.7	3343.1 ± 0.5
		Cd_3-βSpMTB (40)	3280.5	3280.8 ± 0.3

[a] MT concentration and metal/MT ratio calculated from acid ICP-AES results.
[b] Experimental and theoretical molecular weights corresponding to the Zn- and Cd-peptides. Zn and Cd contents were calculated from the mass difference between holo- and apoproteins. Species shown in bold correspond to the major components of the preparations.

very minor Cd_7S_1 species was identified in the Cd-SpMTA preparation (Table 2, Fig. 4(A)), its relative abundance is practically negligible if compared with the minor forms detected in Cd-SpMTB (Fig. 4(D)). In this case, an unexpected major Cd_8 species was produced, together with several significantly abundant minor species, among which Cd_7- and Cd_7S_2-SpMTB are worth noting (Table 2, Fig. 4(D)). The CD fingerprint of this preparation differs from that of Cd-SpMTA, being significantly less intense and confirming the presence of sulfide ligands through the existence of the negative band at 280 nm (Fig. 5(A)). The occurrence of numerous species in the recombinant Cd-SpMTB preparation, some of which have a clear sulfide content, is again indicative of a low Cd^{II}-binding ability of SpMTB, as occurred for Zn(II) ions, according to the criteria reported by our group to differentiate MT peptides exhibiting either divalent or monovalent metal ion coordination preference [3].

The Zn(II) and Cd(II) binding abilities of the separate α domains appeared identical for both isoforms, generating almost single Zn_4 and Cd_4 species (Figs. 2(B) and (E), and 4(B) and (E), respectively, and Table 2), also with similar CD fingerprints (Figs. 3(B) and 5(B)). In the case of Cd_4-αSpMTA, the spectrum fully coincides with that previously reported after subtilisin digestion of the complete Cd_7-SpMTA complex [14]. Moreover, this spectrum can be also obtained by Zn/Cd replacement after the addition of 4 Cd(II) equivalents to Zn_4-αSpMTA at pH 7 (Fig. 6). In contrast to these results, the βSpMTA and βSpMTB domains yield patently different results when synthesized in Zn(II)- and Cd(II)-enriched media. Hence, both isoforms are recovered as major Zn_3 complexes, although the partially undermetalated species detectable for SpMTA do not appear for SpMTB (Table 2, Fig. 2(C) and (F)). Also, as determined from the difference between conventional and acid ICP-AES measurements (data not shown), the presence of inorganic sulfide in the recombinant Zn-βSpMTB preparations may account for the red-shift observed for Zn-βSpMTB CD spectrum in comparison to Zn-βSpMTA (Fig. 3(C)). Even more pronounced differences arise for the Cd^{II}-binding capacity of the separate β domains, as βSpMTA yields a major, canonical Cd_3 species accompanied by minor Zn-containing complexes, while βSpMTB predominantly folds into Cd_3S_2-βSpMTB, thus with complete absence of Zn (Fig. 4(C) and (F), respectively, and Table 2). Moreover, the Cd_3S_2-βSpMTB sulfide containing complex exhibits an acute red-shift in its CD spectrum when compared to Cd_3-βSpMTA (Fig. 5(C)).

At this point, it becomes evident that the Cd-binding abilities of SpMTB are poorer than those of SpMTA [3], and that this feature is most likely due to a patent lower M^{II}-binding ability of βSpMTB if compared to βSpMTA, as corroborated by the fact that the respective α domains exhibit no major differences. In order to better understand the peculiarities of the Cd-SpMTA and Cd-SpMTB complexes, and to support the higher M^{II}-binding preference of βSpMTA compared to βSpMTB, additional experimental results were considered. In the first place, it is worth noting that the CD spectra of the Zn/Cd replacement processes in both β domains evolved following a distinct pattern,

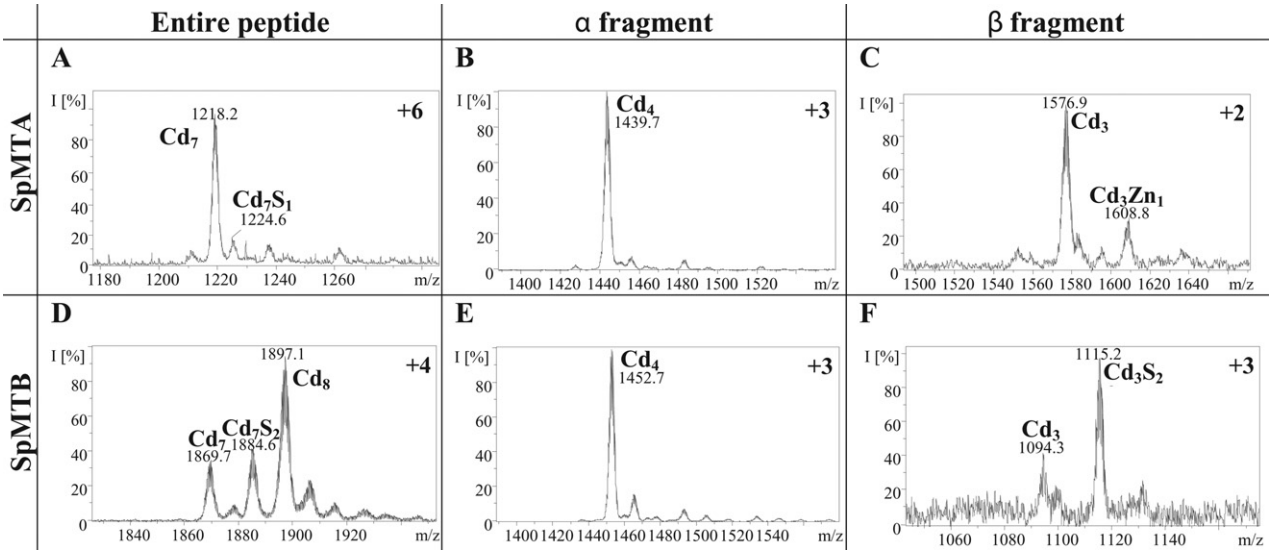

Fig. 4. Representative charge states for the ESI-MS spectra recorded at pH 7.0 of recombinant Cd-SpMTA (A), Cd-αSpMTA (B), Cd-βSpMTA (C), Cd-SpMTB (D), Cd-αSpMTB (E) and Cd-βSpMTB (F). The observed species are collected in Table 2.

Table 3
Analytical characterization of recombinant SpMTA and its independent constitutive fragments synthesized in Cu-enriched media under normal (N.A.) and low (L.A.) aeration conditions.

MT	Concentration and metal/MT ratio[a]	ESI-MS[b]			
			Species (% abundance)	Theoretical MW	Experimental MW
SpMTA (N.A.)	0.5 × 10^{-4} M	pH 7.0	**M_4-SpMTA (100)**	6782.7–6786.0	6771.0 ± 0.1
	5.5 Cu		M_8-SpMTA (80)	7032.8–7039.5	7029.7 ± 1.2
	3.0 Zn		M_5-SpMTA (40)	6845.2–6849.4	6838.0 ± 1.1
			M_9-SpMTA (40)	7095.3–7102.9	7092.5 ± 1.5
			M_6-SpMTA (30)	6907.7–6912.8	6899.8 ± 1.3
		pH 2.5	**Cu_4-SpMTA (100)**	6782.7	6773.5 ± 0.5
			Cu_8-SpMTA (20)	7032.8	7035.3 ± 2.2
			Apo-SpMTA (20)	6532.0	6522.5 ± 2.3
SpMTA (L.A.)	0.5 × 10^{-4} M	pH 7.0	**M_8-SpMTA (100)**	7032.8–7039.5	7030.6 ± 0.8
	8.7 Cu		M_{11}-SpMTA (60)	7220.4–7229.6	7224.6 ± 0.3
	1.7 Zn		M_9-SpMTA (60)	7095.3–7102.9	7096.8 ± 1.0
			M_{10}-SpMTA (40)	7157.9–7166.2	7161.4 ± 1.2
		pH 2.5	**Cu_8-SpMTA (100)**	7032.8	7029.1 ± 1.2
			Cu_9-SpMTA (40)	7095.3	7094.1 ± 1.8
αSpMTA (N.A.)	0.3 × 10^{-4} M	pH 7.0	Oxidized dimeric species	–	–
	6.0 Cu	pH 2.5	N.D.	–	–
	0.1 Zn				
αSpMTA (L.A.)	0.2 × 10^{-4} M	pH 7.0	N.D.	–	–
	4.2 Cu	pH 2.5	Oxidized dimeric species	–	–
	0.2 Zn				
βSpMTA (N.A.)	0.7 × 10^{-4} M	pH 7.0	**M_5-βSpMTA (100)**	3132.9–3137.1	3129.6 ± 0.1
	5.1 Cu		M_6-βSpMTA (30)	3195.5–3200.5	3195.6 ± 0.3
	0.2 Zn		M_4-βSpMTA (20)	3070.4–3073.7	3067.6 ± 2.1
			M_7-βSpMTA (20)	3258.0–3263.8	3255.4 ± 1.9
		pH 2.5	N.D.	–	–
βSpMTA (L.A.)	0.05 × 10^{-4} M	pH 7.0	**M_5-βSpMTA (100)**	3132.9–3137.1	3131.6 ± 1.6
	3.4 Cu		M_4-βSpMTA (40)	3070.4–3073.7	3066.8 ± 1.9
	0.7 Zn	pH 2.5	N.D.	–	–

[a] MT concentration and metal/MT ratio calculated from acid ICP-AES results.
[b] Experimental and theoretical molecular weights corresponding to the Cu-peptides. Species shown in bold correspond to the major components of the preparations. In the case of Zn, Cu mixed-metal species, the indicated theoretical molecular weights correspond to the homometallic Cu_x and Zn_x species ($MW_{Cu\text{-}MT}$–$MW_{Zn\text{-}MT}$), and the metal-to-protein stoichiometries deduced at pH 7.0 are indicated as M_x (M = Zn + Cu). Cu contents at pH 2.5 were calculated from the mass difference between holo- and apoproteins. N.D.: not detected.

Table 4
Analytical characterization of recombinant SpMTB and its independent constitutive fragments synthesized in Cu-enriched media under normal (N.A.) and low (L.A.) aeration conditions.

MT	Concentration and metal/MT ratio[a]	ESI-MS[b]			
		Species (% abundance)		Theoretical MW	Experimental MW
SpMTB (N.A.)	0.9 × 10^{-4} M 5.5 Cu 1.9 Zn	pH 7.0	**M_8-SpMTB (100)**	7201.1–7207.8	7196.1 ± 0.6
			M_{10}-SpMTB (70)	7326.2–7334.6	7322.8 ± 1.0
			M_9-SpMTB (60)	7263.7–7271.2	7260.8 ± 0.9
			M_{11}-SpMTB (20)	7388.8–7398.0	7387.6 ± 0.7
			M_5-SpMTB (20)	7013.5–7017.7	7002.8 ± 1.1
		pH 2.5	**Cu_8-SpMTB (100)**	7201.1	7196.0 ± 0.1
			Cu_4-SpMTB (40)	6950.9	6944.6 ± 1.1
			Cu_9-SpMTB (40)	7263.7	7261.0 ± 1.2
			Cu_5-SpMTB (20)	7013.5	7008.0 ± 1.6
SpMTB (L.A.)	0.2 × 10^{-4} M 14.5 Cu 0.0 Zn	pH 7.0 and 2.5	N.D.	–	–
αSpMTB (N.A.)	0.6 × 10^{-4} M 5.5 Cu 0.5 Zn	pH 7.0	**M_5-αSpMTB (100)**	4226.2–4230.5	4223.0 ± 1.0
			M_4-αSpMTB (70)	4163.7–4167.1	4159.2 ± 1.1
			M_7-αSpMTB (60)	4351.3–4357.2	4350.0 ± 0.7
		pH 2.5	**Cu_4-αSpMTB (100)**	4163.7	4158.6 ± 0.6
			Cu_5-αSpMTB (80)	4226.2	4222.0 ± 0.9
			Cu_7-αSpMTB (40)	4351.3	4348.0 ± 1.2
αSpMTB (L.A.)	0.3 × 10^{-4} M 7.0 Cu 0.0 Zn	pH 7.0	N.D.	–	–
		pH 2.5	**Cu_4-αSpMTB (100)**	4163.7	4157.6 ± 0.5
			Cu_5-αSpMTB (90)	4226.2	4221.9 ± 0.9
			Apo-αSpMTB (90)	3913.5	3903.3 ± 0.1
βSpMTB (N.A.)	0.3 × 10^{-4} M 3.3 Cu 0.2 Zn	pH 7.0	**M_5-βSpMTB (100)**	3262.0–3266.3	3260.2 ± 0.4
			M_7-βSpMTB (80)	3387.1–3393.0	3386.6 ± 0.8
			M_8-βSpMTB (80)	3449.7–3456.4	3449.0 ± 0.5
			M_6-βSpMTB (40)	3324.6–3329.6	3322.6 ± 1.0
		pH 2.5	**Cu_8-βSpMTB (100)**	3449.7	3448.5 ± 0.1
			Apo-βSpMTB (100)	2949.3	2940.9 ± 1.2
			Cu_4-βSpMTB (60)	3199.5	3195.3 ± 0.6
			Cu_5-βSpMTB (60)	3262.0	3259.7 ± 1.0
			Cu_7-βSpMTB (60)	3387.1	3385.5 ± 0.1
βSpMTB (L.A.)	N.D.	pH 7.0 and 2.5	N.D.	–	–

[a] MT concentration and metal/MT ratio calculated from acid ICP-AES results.
[b] Experimental and theoretical molecular weights corresponding to the Cu-peptides. Species shown in bold correspond to the major components of the preparations. In the case of Zn, Cu mixed-metal species, the indicated theoretical molecular weights correspond to the homometallic Cu_x and Zn_x species ($MW_{Cu\text{-}MT}$–$MW_{Zn\text{-}MT}$), and the metal-to-protein stoichiometries deduced at pH 7.0 are indicated as M_x (M = Zn + Cu). Cu contents at pH 2.5 were calculated from the mass difference between holo- and apoproteins. N.D.: not detected.

especially after the 3rd Cd(II) equivalent added (Fig. 7(A)–(D)). But most interestingly, while the CD fingerprint of the recombinant Cd-βSpMTA preparation was reproduced after the 3rd Cd(II) equivalent added to Zn-βSpMTA (Fig. 7(E)), this was not the case for βSpMTB, even after the addition of 1–3 Na_2S equivalents, which provoked the conversion of the derivative-shaped band into a Gaussian band (Fig. 7(F)). For the Cd-βMTB isoform, the initial CD fingerprint can only be recovered after an acidification/reneutralization process followed by addition of 3 S^{2-} equivalents (Fig. 7(G)). Taken together, these data confirm that βSpMTB shows a diminished preference for divalent metal ion binding than βSpMTA, as highlighted by the need of S^{2-} ions in order to stabilize its M(II)-recombinant forms, and it is likely that the β moiety somehow confers its character to the entire SpMTB protein, which behaves as a less proficient Cd(II)-binding peptide. Since the analysis of the metal-binding behavior of a considerable number of MTs has revealed that the decrease of the divalent metal ion-preference (Zn(II) or Cd(II)) of an MT peptide entails the increase of its monovalent metal ion-preference (Cu(I)) and *vice versa* [3], it was plausible to hypothesize that SpMTB would exhibit a more accentuated Cu-thionein character than SpMTA. Thus, we thoroughly considered the results of recombinantly synthesizing both isoforms, and their independent domains, in copper-supplemented *E. coli* cells.

3.3. Cu-binding abilities: SpMTB exhibits a stronger Cu-thionein character than SpMTA

Two different types of preparations were obtained for SpMTA when synthesized in Cu-supplemented *E. coli* cells, depending on the aeration conditions of the corresponding bacterial cultures (*cf.* Table 3). Although in both cases SpMTA was recovered as a mixture of Zn, Cu heteronuclear species, the average Zn content of the preparation was always higher in the normally aerated culture, with concomitant average lower Cu content (5.5 Cu:3.0 Zn), and with the opposite results for the low aeration conditions (8.7 Cu:1.7 Zn). In concordance with these ICP-AES results, in the former case the most abundant detected species by ESI-MS was M_4-SpMTA, followed by a collection of higher nuclearity complexes (M_5–M_9, Fig. 8(A)), which should be mainly consisting of Cu_4Zn_x complexes ($1 < x < 5$), since ESI-MS data at pH 2.5 identified a highly predominant Cu_4 cluster (Fig. 8(B)). Conversely, when SpMTA was synthesized under low aeration, the most abundant species in solution switched to M_8 (M = Zn + Cu), readily followed by M_9–M_{11} complexes (Fig. 8(C)), whose acid ESI-MS analyses revealed to be built by Cu_8 and Cu_9 cores (Fig. 8(D)) plus some added Zn(II) ions. The homologous SpMTB was also synthesized under both culture conditions. Under normal aeration, this isoform yielded preparations similar to those of SpMTA when produced under low aeration, *i.e.* a predominant M_8 complex accompanied by M_9 and M_{10} species that acid ESI-MS identified as predominant Cu_8Zn_y complexes (Table 4, Fig. 8(E) and (F)). With respect to the recombinant

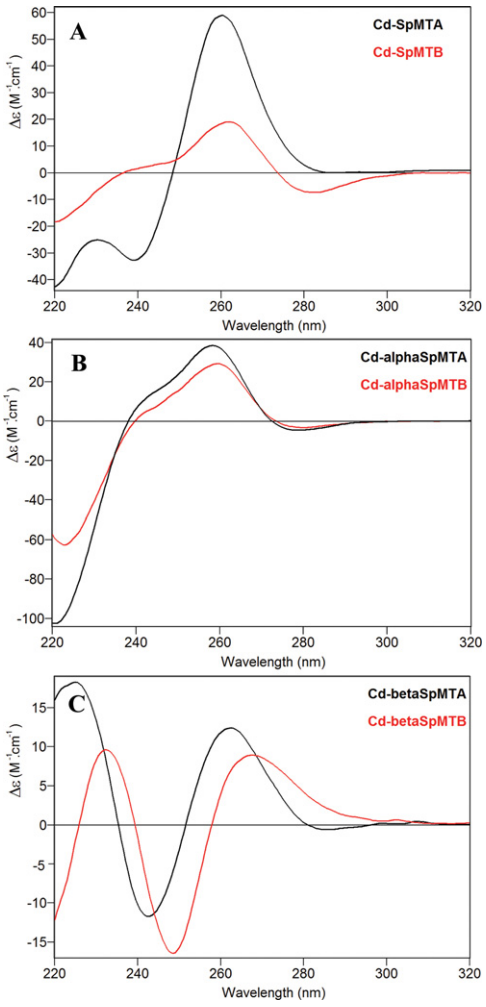

Fig. 5. CD spectra corresponding to the entire MT (A) and the separate constitutive α (B) and β (C) domains of SpMTA (black) and SpMTB (red) recombinantly synthesized in Cd-supplemented media. (For interpretation of the references to color in this figure legend, the reader is referred to the web version of this article.)

Cu-SpMTB synthesis at low aeration, ICP-AES results indicate the formation of homometallic Cu species (average metal content of 14.5 Cu/MT and absence of Zn(II) ions, Table 4). Unfortunately, due to the low concentration of the sample, possibly due to an intrinsic poor folding of these complexes (as pointed out by their CD spectra, Fig. 9), ESI-MS detection of the corresponding species was repeatedly unsuccessful. Since the less aerated an *E. coli* culture, the higher the Cu content of the grown cells, it is obvious that the capacity of SpMTB to exhibit, even under lower Cu assayed concentrations, the Cu(I)-binding behavior that SpMTA is only able to perform in the presence of higher copper amounts, argues in favor of the increased Cu-thionein character of the former. It is worth noting that the major stoichiometries reported here for both SpMT isoforms (*i.e.* Cu_4Zn_x and Cu_8Zn_y) have also been reported for mammalian MT1 [24,25] and MT3 [26], mussel Me-MT-10-IV [20], or nematode CeMT1 and CeMT2 [27], this indicating that this set of approximately 60-residue MTs commonly fold into clusters containing a multiple of 4 Cu(I) ions complemented with a variable number of Zn(II) ions.

Again, the characterization of the Cu(I) binding abilities of the separate domains of both SpMT isoforms proved to be a valuable tool to confirm and further analyze the higher Cu-thionein character of SpMTB regarding SpMTA. First unforeseen information was that both α moieties showed distinct Cu(I) binding behavior, contrarily to what was observed for divalent metal ions. Hence, αSpMTA yielded, under all assay conditions, mixtures of Zn, Cu heterometallic complexes with highly oxidized and/or poorly metalated species, together with dimeric complexes (Table 3), which exhibit almost flat CD fingerprints (Fig. 9(C) and (D)). Contrarily, αSpMTB invariably yielded well defined results: at regular oxygenation Cu_5-, Cu_4Zn_1-, Cu_4- and Cu_7-αSpMTB were the predominant species (Fig. 10(A) and (D), Table 4), and at low aeration conditions a mixture of homometallic Cu complexes with major Cu_4 and Cu_5 stoichiometries was detected (Fig. 10(F), Table 4). These results were consistent with well-defined CD spectra, typical of Cu-MT chromophores, despite the fact that they exhibited rather low intensity (Fig. 9(C) and (D)). Contrarily to the α domains, no significant differences could be detected for the recombinantly synthesized β peptides in copper-supplemented media. At normal aeration both isoforms yield a mixture of species with close average Zn/MT (0.2) and Cu/MT (3.3–5.1) ratios (Tables 3 and 4) and very similar CD spectra (Fig. 9(E)), where M_5 is the major species present (Fig. 10(B) and (C)). ESI-MS at pH 2.5 (Fig. 10(E)) confirmed the almost quasi homometallic nature of the Cu-βSpMTB preparations, and comparison with data at pH 7.0 allowed to deduce that the M_5 major species corresponds to a mixture of Cu_5 and Cu_4Zn_1 complexes. At low aeration, very diluted samples were obtained and consequently very weak CD spectra were recorded (Fig. 9(F)). However, βSpMTA ESI-MS analysis at pH 7.0 (Fig. 10(G)) shows a heterometallic species distribution similar to that observed at normal oxygenation, with a major M_5 form (Table 3). In view of the results obtained in the recombinant syntheses of the βSpMT fragments, and in order to have a more precise picture of their differential behavior when coordinating Cu(I), Zn/Cu titrations were performed and followed through their CD spectra evolution. In the case of βSpMTA, the maximum degree of folding was achieved for 3–4 Cu(I) equivalents added to the Zn(II)-βSpMTA preparation, with little further variation (Fig. 11(A)–(C)). Contrastingly, βSpMTB reaches its maximum folding after 6 Cu(I) equivalents added (Fig. 11(D)–(F)), which is in concordance with a greater Cu(I) binding capacity. Finally, when comparing these results with those of the recombinant complexes, it becomes obvious that the CD spectrum of βSpMTA is fully reproduced after 4 Cu(I) equivalents added (Fig. 11(G)), whereas for βSpMTB, the highest CD spectra resemblance is attained after 7 Cu(I) equivalents added (Fig. 11(H)).

4. Conclusions

From the set of data reported in this work, a differential metal ion binding preference is envisaged for SpMTA and SpMTB, since different results attribute a more pronounced Cu-thionein character to SpMTB than to SpMTA, and *vice versa* for the Zn(II) and Cd(II)-thionein character. In summary, and according to the criteria proposed to evaluate the preference of a given MT peptide either for monovalent or divalent metal ion coordination [3], it is worth noting that (i) SpMTA is able to fold into almost unique and sulfide-free Zn(II) or Cd(II)-complexes, while for these metal ions SpMTB yields preparations containing a large variety of species, and with a significant sulfide content; and (ii) SpMTB is able to yield, at standard bacterial cell copper concentrations (*i.e.* normal aeration of the *E. coli* cultures), Cu-complexes that SpMTA is only able to produce in higher-copper environments. Dissection of the metal-binding abilities of both isoforms into their domains suggests that while the β domain would be the only one responsible for the diminished divalent metal binding capacity of SpMTB, both domains would contribute to the enhanced capacity of SpMTB for Cu(I) binding.

The differential Zn/Cu binding performance of SpMTA and SpMTB suggests that both isoforms exert at least partially distinct complementary functions in the physiology of sea urchins. For divalent metal ions, SpMTA may be mostly responsible for housekeeping Zn homeostasis, while SpMTB would only come into play under Zn or Cd overload emergency situations. This hypothesis is supported by the fact

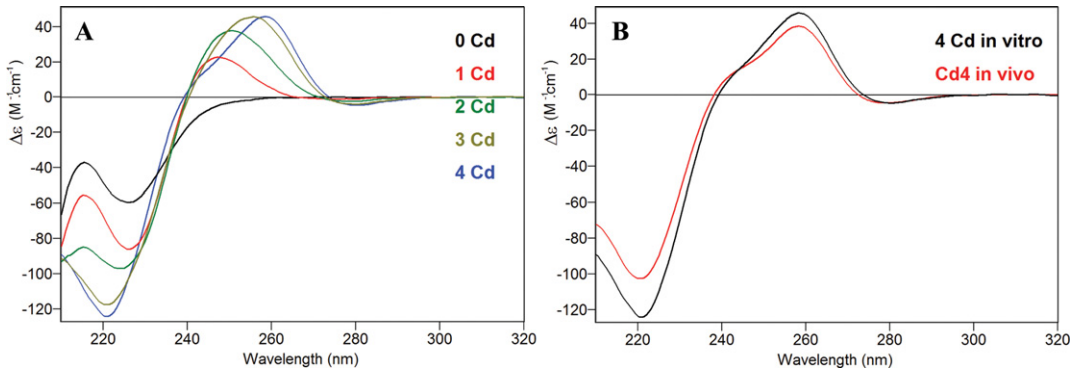

Fig. 6. CD spectra recorded during the titration of Zn_4-αSpMTA with Cd(II) at pH 7 (A) and superimposition of CD spectra of Cd_4-αSpMTA obtained by Zn/Cd substitution over Zn_4-αSpMTA (*in vitro*; black) and by recombinant synthesis in Cd-enriched media (*in vivo*; red) (B). (For interpretation of the references to color in this figure legend, the reader is referred to the web version of this article.)

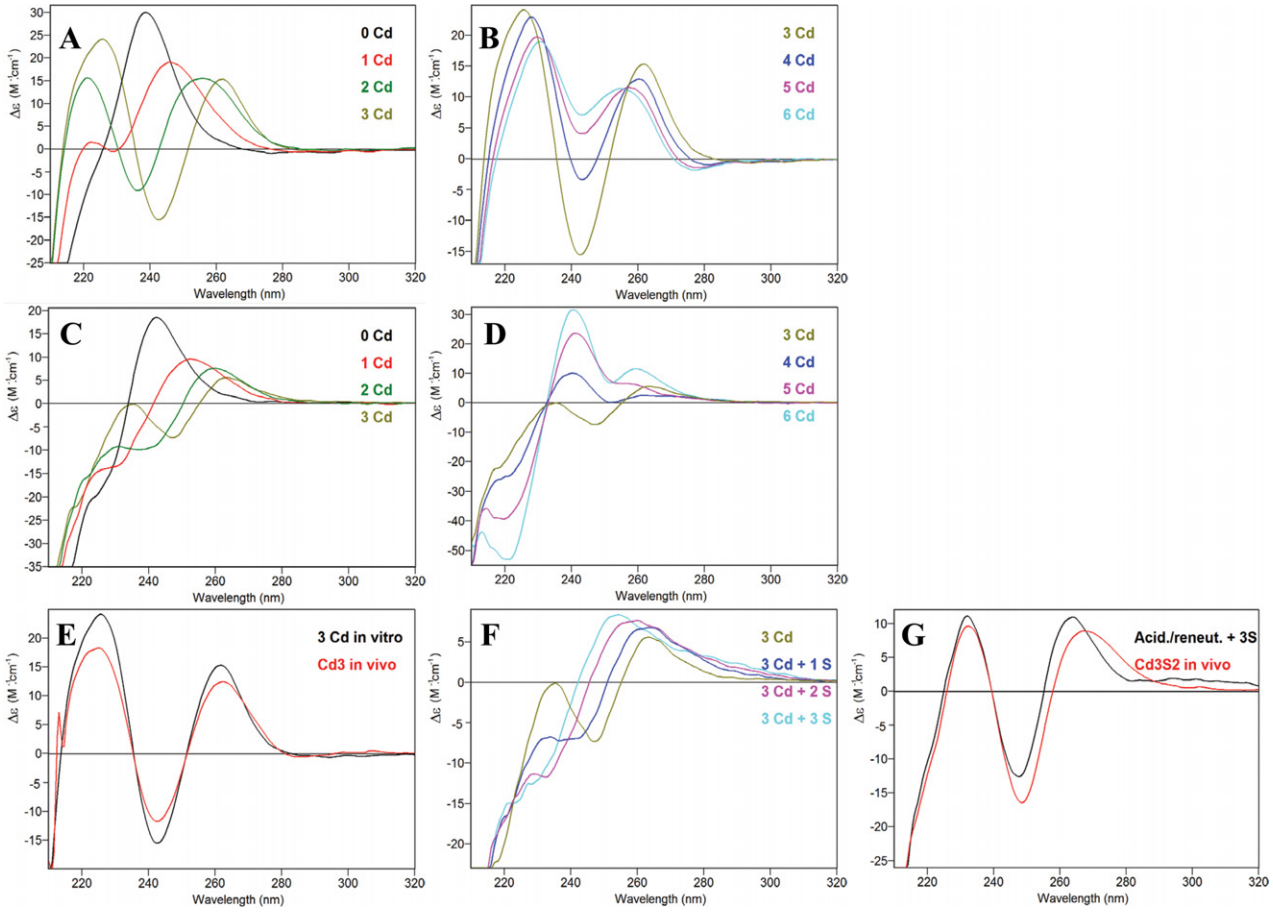

Fig. 7. CD spectra recorded during the titrations of Zn-βSpMTA (A, B) and Zn-βSpMTB (C, D) with Cd(II) at pH 7. The effect of the addition of S^{2-} to βSpMTB is also shown (F), as well as the CD superimposition of *in vivo* (red) and *in vitro* (black) Cd-βSpMTA (E) and Cd-βSpMTB (G) species obtained after addition of 3 Cd(II) equivalents to Zn-βSpMTA or after an acidification/reneutralization process of Cd-βSpMTB plus addition of 3 S^{2-} equivalents. (For interpretation of the references to color in this figure legend, the reader is referred to the web version of this article.)

that *SpMTA* is constitutively expressed at a higher rate than *SpMTB* at low Zn concentrations, while increased divalent metal ion concentrations induce *SpMTB* expression up to similar values than *SpMTA* [8], analogously to what has been described for the nematode CeMT1 and CeMT2 isoforms [27]. Interestingly, the existence of multiple MT isoforms involved in different physiological roles has been very recently confirmed in another sea urchin species, *Paracentrotus lividus*, in which its five different MT isogenes respond disctinctively to Cd transcriptional activation, thus showing a certain degree of evolutive functional differentiation [28]. Unfortunately, no information is available for the copper physiology in sea urchin, or for copper requirements during its development stages, or for the response of both *SpMT* isogenes to copper overload. It would not be far-fetched to assume that SpMTB, given its higher Cu-thionein character, could better perform some function related to Cu metabolism in this group of organisms. Overall, and as for other taxa in which MT peptides have

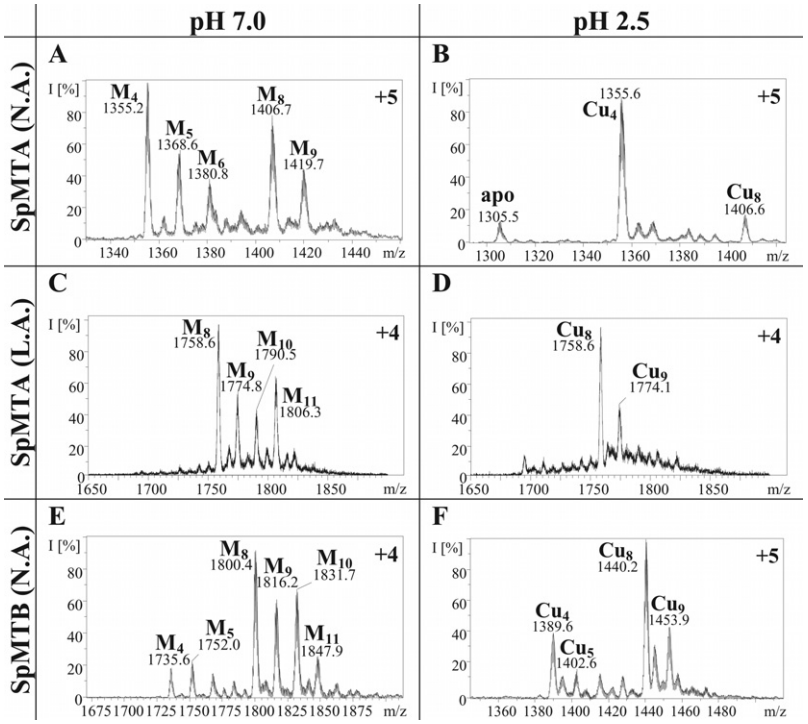

Fig. 8. Representative charge states for the ESI-MS spectra recorded at pH 7.0 and pH 2.5 of recombinant SpMTA (A, B) and SpMTB (E, F) synthesized in Cu-supplemented *E. coli* media at normal aeration (N.A.) conditions, and of recombinant Cu-SpMTA (C, D) obtained at low aeration (L.A.) conditions. The observed species are collected in Tables 3 and 4.

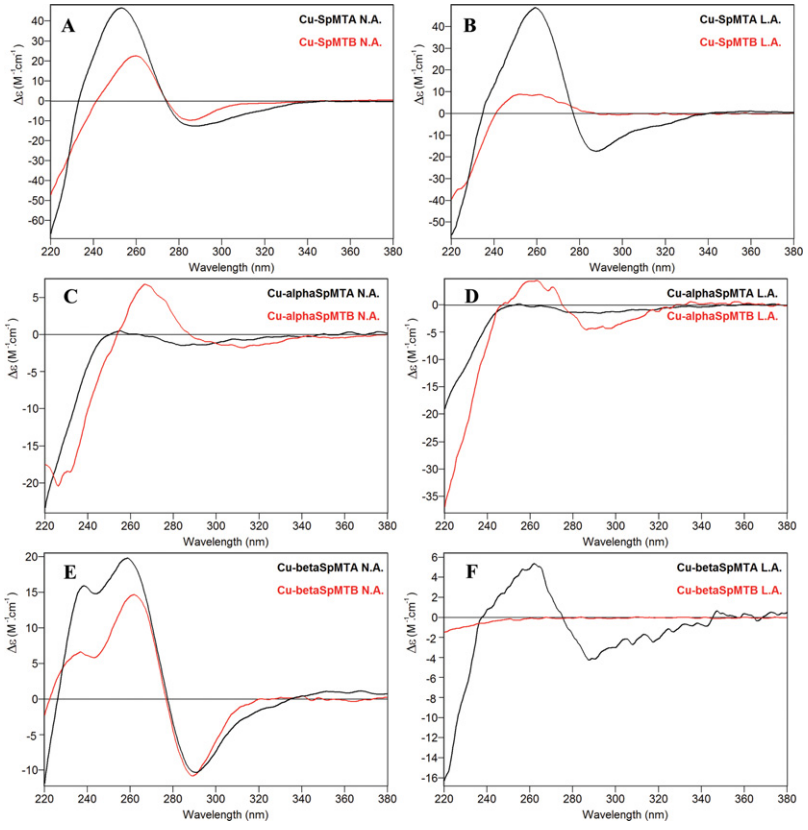

Fig. 9. CD spectra corresponding to the entire MT (A, B) and the separate constitutive α (C, D) and β (E, F) domains of SpMTA (black) and SpMTB (red) recombinantly synthesized in Cu-supplemented media at normal aeration (N.A.) and low aeration (L.A.) conditions (left and right, respectively). (For interpretation of the references to color in this figure legend, the reader is referred to the web version of this article.)

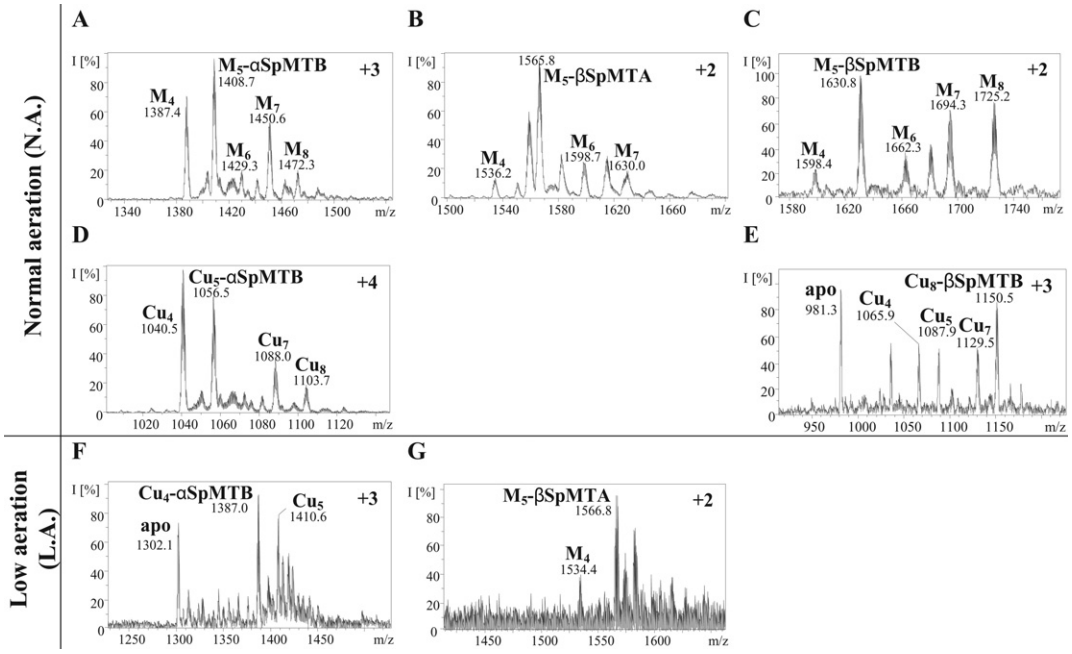

Fig. 10. Representative charge states for the ESI-MS spectra of recombinant αSpMTB (A, D, F), βSpMTA (B, G) and βSpMTB (C, E) synthesized in Cu-supplemented *E. coli* media at normal (N.A.) and low (L.A.) aeration conditions. M-MT species where M = Zn + Cu are assigned in spectra recorded at pH 7.0 (A–C, G), while Cu-MT species are assigned when recorded at pH 2.5 (D–F). The observed species are collected in Tables 3 and 4.

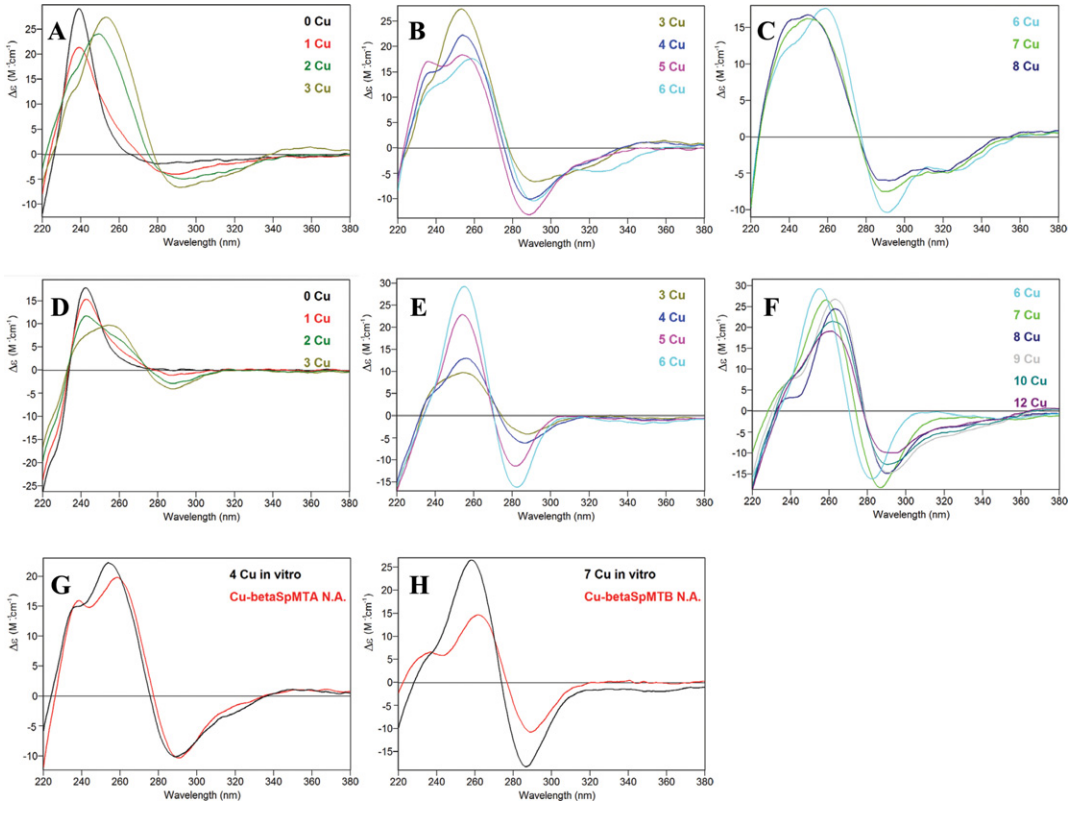

Fig. 11. CD spectra recorded during the titration of Zn-βSpMTA (A–C) and Zn-βSpMTB (D–F) with Cu(I) at pH 7. Also, a comparison with the CD spectrum of the corresponding recombinant Cu-βMT samples obtained at normal aeration conditions (in red) is shown (G, H). (For interpretation of the references to color in this figure legend, the reader is referred to the web version of this article.)

been previously characterized, more or less pronounced differential metal ion binding properties would underlie the observed polymorphism, even when the involved polypeptides share a 85% sequence identity, as is the case for *S. purpuratus* MTs.

Acknowledgements

This work was financially supported by the Spanish *Ministerio de Ciencia e Innovación* grants to the projects BIO2012-39682-C02-01 (S. Atrian) and BIO2012-39682-C02-02 (M. Capdevila). The authors are members of the "Grup de Recerca de la Generalitat de Catalunya" ref. 2009SGR-1457. We thank the *Serveis Científico-Tècnics de la Universitat de Barcelona* and the *Servei d'Anàlisi Química (SAQ) de la Universitat Autònoma de Barcelona* for allocating DNA sequencing, ICP-AES, CD, UV–vis and ESI-MS instrument time.

References

[1] Capdevila M., Bofill R., Palacios O., Atrian S. (2012) State-of-the-art of metallothioneins at the beginning of the 21st century. Coord. Chem. Rev. 256, 46–52.
[2] Valls M., Bofill R., Gonzàlez-Duarte R., Gonzàlez-Duarte P., Capdevila M., Atrian S. (2001) A new insight into MT classification and evolution. The *in vivo* and *in vitro* metal binding features of *Homarus americanus* recombinant MT. J. Biol. Chem. 276, 32835–32843.
[3] Bofill R., Capdevila M., Atrian S. (2009) Independent metal-binding features of recombinant metallothioneins convergently draw a step gradation between Zn- and Cu-thioneins. Metallomics. 1, 229–234.
[4] Palacios O., Pagani A., Pérez-Rafael S., Egg M., Höckner M., Brandstätter A. et al. (2011) Shaping mechanisms of metal specificity in a family of metazoan metallothioneins: evolutionary differentiation of mollusc metallothioneins. BMC Biol. 9, 4.
[5] Capdevila M., Atrian S. (2011) Metallothionein protein evolution: a miniassay. J. Biol. Inorg. Chem. 16, 977–989.
[6] Palacios O., Atrian S., Capdevila M. (2011) Zn- and Cu-thioneins: a functional classification for metallothioneins? J. Biol. Inorg. Chem. 16, 991–1009.
[7] Vergani L. (2009) Metallohioneins from echinoderms. In: A. Sigel, H. Sigel, R.K.O. Sigel (Eds.), Metal Ions in Life Sciences 5: Metallothioneins and Related Chelators. Cambridge: Royal Society of Chemistry, pp. 228–237.
[8] Wilkinson D.G., Nemer M. (1987) Metallothionein genes MTa and MTb expressed under distinct quantitative and tissue-specific regulation in sea urchin embryos. Mol. Cell. Biol. 7, 48–58.
[9] Harlow P., Watkins E., Thorton R.D., Nemer M. (1989) Structure of an ectodermally sea urchin metallothionein gene and characterization of its metal-responsive region. Mol. Cell. Biol. 9, 5445–5455.
[10] Nemer M., Thornton R.D., Stuebing E.W., Harlow P. (1991) Structure, spatial and temporal expression of two sea urchin metallothionein genes, $SpMTB_1$ and $SpMTA^*$. J. Biol. Chem. 266, 6586–6593.
[11] Nemer M., Wilkinson D.G., Travaglini E.C., Sternberg E.J., Butt T.R. (1985) Sea urchin metallothionein sequence: key to an evolutionary diversity. Proc. Natl. Acad. Sci. USA. 82, 4992–4994.
[12] Wang Y., Mackay E.A., Kurasaki M., Kägi J.H.R. (1994) Purification and characterisation of recombinant sea urchin metallothionein expressed in *Escherichia coli*. Eur. J. Biochem. 225, 449–457.
[13] Wang Y., Mackay E.A., Zerbe O., Hess D., Hunziker P.E., Vašák M. et al. (1995) Characterization and sequential localization of the metal clusters in sea urchin metallothionein. Biochemistry. 34, 7460–7467.
[14] Wang Y., Hess D., Hunziker P.E., Kägi J.H.R. (1996) Separation and characterization of the metal–thiolate-cluster domains of recombinant sea urchin metallothionein. Eur. J. Biochem. 241, 835–839.
[15] Riek R., Prêcheur B., Wang Y., Mackay E.A., Wider G., Guntert P. et al. (1999) NMR structure of the sea urchin (*Strongylocentrotus purpuratus*) metallothionein MTA. J. Mol. Biol. 291, 417–428.
[16] Capdevila M., Cols N., Romero-Isart N., Gonzàlez-Duarte R., Atrian S., Gonzàlez-Duarte P. (1997) Recombinant synthesis of mouse Zn_3-beta and Zn_4-alpha metallothionein 1 domains and characterization of their cadmium(II) binding capacity. Cell. Mol. Life Sci. 53, 681–688.
[17] Cols N., Romero-Isart N., Capdevila M., Oliva B., Gonzàlez-Duarte P., Gonzàlez-Duarte R. et al. (1997) Binding of excess cadmium(II) to Cd_7-metallothionein from recombinant mouse Zn_7-metallothionein 1. UV–VIS absorption and circular dichroism studies and theoretical location approach by surface accessibility analysis. J. Inorg. Biochem. 68, 157–166.
[18] Pagani A., Villarreal L., Capdevila M., Atrian S. (2007) The *Saccharomyces cerevisiae* Crs5 metallothionein metal-binding abilities and its role in the response to zinc overload. Mol. Microbiol. 63, 256–269.
[19] Bofill R., Palacios O., Capdevila M., Cols N., Gonzàlez-Duarte R., Atrian S. et al. (1999) A new insight into the Ag^+ and Cu^+ binding sites in the metallothionein beta domain. J. Inorg. Biochem. 73, 57–64.
[20] Orihuela R., Domènech J., Bofill R., You C., Mackay E.A., Kägi J.H.R. et al. (2008) The metal-binding features of the recombinant mussel *Mytilus edulis* MT-10-IV metallothionein. J. Biol. Inorg. Chem. 13, 801–812.
[21] Domènech J., Orihuela R., Mir G., Molinas M., Atrian S., Capdevila M. (2007) The Cd(II)-binding abilities of recombinant *Quercus suber* metallothionein: bridging the gap between phytochelatins and metallothioneins. J. Biol. Inorg. Chem. 12, 867–882.
[22] Bongers J., Walton C.D., Richardson D.E., Bell J.U. (1988) Micromolar protein concentrations and metalloprotein stoichiometries obtained by inductively coupled plasma atomic emission spectrometric determination of sulfur. Anal. Chem. 60, 2683–2686.
[23] Capdevila M., Domènech J., Pagani A., Tío L., Villarreal L., Atrian S. (2005) Zn- and Cd-metallothionein recombinant species from the most diverse phyla may contain sulfide (S^{2-}) ligands. Angew. Chem. Int. Ed. Engl. 44, 4618–4622.
[24] Jensen L.T., Peltier J.M., Winge D.R. (1998) Identification of a four copper folding intermediate in mammalian copper metallothionein by electrospray ionization mass spectrometry. J. Biol. Inorg. Chem. 3, 627–631.
[25] Dolderer B., Echner H., Beck A., Hartmann H.J., Weser U., Luchinat C. et al. (2007) Coordination of three and four Cu(I) to the alpha- and beta-domain of vertebrate Zn-metallothionein-1, respectively, induces significant structural changes. FEBS J. 274, 2349–2362.
[26] Bogumil R., Faller P., Pountney D.L., Vašák M. (1996) Evidence for Cu(I) clusters and Zn(II) clusters in neuronal growth-inhibitory factor isolated from bovine brain. Eur. J. Biochem. 238, 698–705.
[27] Bofill R., Orihuela R., Romagosa M., Domènech J., Atrian S., Capdevila M. (2009) *Caenorhabditis elegans* metallothionein isoform specificity: metal binding abilities and the role of histidine in CeMT1 and CeMT2. FEBS J. 276, 7040–7056.
[28] Ragusa M.A., Costa S., Gianguzza M., Roccheri M.C., Gianguzza F. (2012) Effects of cadmium exposure on sea urchin development assessed by SSH and RT-qPCR: metallothionein genes and their differential induction. Mol. Biol. Rep http://dx.doi.org/10.1007/s11033-012-2275-7.